Towards understanding the difference of optoelectronic performance between micro- and nanoscale metallic layers

MIKITA MARUS,[1] ALIAKSANDR HUBAREVICH,[1] HONG WANG,[1] YAUHEN MUKHA,[2] ALIAKSANDR SMIRNOV,[2] HUI HUANG,[3,5] XIAO WEI SUN,[1,4] AND WEIJUN FAN[1,*]

[1]*School of Electrical and Electronic Engineering, Nanyang Technological University, 50 Nanyang Avenue, 639798, Singapore*
[2]*Department of Micro- and Nano-Electronics, Belarusian State University of Informatics and Radioelectronics, 6 P. Brovki, Minsk 220013, Belarus*
[3]*Singapore Institute of Manufacturing Technology, 71 Nanyang Drive, 638075, Singapore*
[4]*Department of Electrical and Electronic Engineering, College of Engineering, South University of Science and Technology, 1088 Xue-Yuan Road, Nanshan, Shenzhen, Guangdong 518055, China*
[5]*HHUANG@simtech.a-star.edu.sg*
**EWJFAN@ntu.edu.sg*

Abstract: Optoelectronic performance of nano-/microscale porous and wired silver (*Ag*) and aluminum (*Al*) layers was theoretically studied. Within the *nanoscale* region, *Ag* porous and wired layers – possessing stronger surface plasmon response over the whole visible spectrum –demonstrate up to a 20% higher average transmittance in comparison to identic *Al* design. In the *microscale* region, difference in the average transmittance between the above mentioned metallic layers decreases to 5%. Moreover, the *microscale Ag* and *Al* layers exhibit up to a 5% higher average transmittance. The obtained results allow deeper analysis of the pattern scale of metallic transparent conductive layers for various optoelectronic applications, such as displays, solar cells, light-emitting diodes, touch screens and smart windows.

OCIS codes: (310.7005) Transparent conductive coatings; (350.4238) Nanophotonics and photonic crystals.

References and links

1. S. Kang, T. Kim, S. Cho, Y. Lee, A. Choe, B. Walker, S.-J. Ko, J. Y. Kim, and H. Ko, "Capillary printing of highly aligned silver nanowire transparent electrodes for high-performance optoelectronic devices," Nano Lett. **15**(12), 7933–7942 (2015).
2. D. Paeng, J. H. Yoo, J. Yeo, D. Lee, E. Kim, S. H. Ko, and C. P. Grigoropoulos, "Low-cost facile fabrication of flexible transparent copper electrodes by nanosecond laser ablation," Adv. Mater. **27**(17), 2762–2767 (2015).
3. P. B. Catrysse and S. Fan, "Nanopatterned metallic films for use as transparent conductive electrodes in optoelectronic devices," Nano Lett. **10**(8), 2944–2949 (2010).
4. H. Lee, S. Hong, K. Yang, and K. Choi, "Fabrication of 100nm metal lines on flexible plastic substrate using ultraviolet curing nanoimprint lithography," Appl. Phys. Lett. **88**(14), 143112 (2006).
5. M. Layani, A. Kamyshny, and S. Magdassi, "Transparent conductors composed of nanomaterials," Nanoscale **6**(11), 5581–5591 (2014).
6. A. Hubarevich, M. Marus, A. Stsiapanau, A. Smirnov, J. Zhao, W. Fan, H. Wang, and X. Sun, "Transparent conductive nanoporous aluminium mesh prepared by electrochemical anodizing," Phys. Status Solidi., A Appl. Mater. Sci. **212**(10), 2174–2178 (2015).
7. G.-J. Jeong, J.-H. Lee, S.-H. Han, W.-Y. Jin, J.-W. Kang, and S.-N. Lee, "Silver nanowires for transparent conductive electrode to GaN-based light-emitting diodes," Appl. Phys. Lett. **106**(3), 031118 (2015).
8. Q. G. Du, K. Sathiyamoorthy, L. P. Zhang, H. V. Demir, C. H. Kam, and X. W. Sun, "A two-dimensional nanopatterned thin metallic transparent conductor with high transparency from the ultraviolet to the infrared," Appl. Phys. Lett. **101**(18), 181112 (2012).
9. J. H. Maurer, L. González-García, B. Reiser, I. Kanelidis, and T. Kraus, "Templated Self-Assembly of Ultrathin Gold Nanowires by Nanoimprinting for Transparent Flexible Electronics," Nano Lett. **16**(5), 2921–2925 (2016).
10. A. Hubarevich, M. Marus, W. Fan, A. Smirnov, X. W. Sun, and H. Wang, "Theoretical comparison of optical and electronic properties of uniformly and randomly arranged nano-porous ultra-thin layers," Opt. Express **23**(14), 17860–17865 (2015).
11. W.-G. Yan, Z.-B. Li, and J.-G. Tian, "Tunable fabrication and optical properties of metal nano hole arrays," J. Nanosci. Nanotechnol. **15**(2), 1704–1707 (2015).

#264791 http://dx.doi.org/10.1364/OME.6.002655
Journal © 2016 Received 9 May 2016; revised 22 Jun 2016; accepted 6 Jul 2016; published 25 Jul 2016

12. M. Marus, A. Hubarevich, H. Wang, A. Smirnov, X. Sun, and W. Fan, "Optoelectronic performance optimization for transparent conductive layers based on randomly arranged silver nanorods," Opt. Express **23**(5), 6209–6214 (2015).
13. A. R. Rathmell, S. M. Bergin, Y. L. Hua, Z. Y. Li, and B. J. Wiley, "The growth mechanism of copper nanowires and their properties in flexible, transparent conducting films," Adv. Mater. **22**(32), 3558–3563 (2010).
14. J. V. Coe, J. M. Heer, S. Teeters-Kennedy, H. Tian, and K. R. Rodriguez, "Extraordinary transmission of metal films with arrays of subwavelength holes," Annu. Rev. Phys. Chem. **59**(1), 179–202 (2008).
15. M. Marus, A. Hubarevich, H. Wang, A. Stsiapanau, A. Smirnov, X. W. Sun, and W. Fan, "Comparative analysis of opto-electronic performance of aluminium and silver nano-porous and nano-wired layers," Opt. Express **23**(20), 26794–26799 (2015).
16. Lumerical FDTD Solutions, Available from: https://www.lumerical.com/tcad-products/fdtd/.
17. B. Last and D. Thouless, "Percolation theory and electrical conductivity," Phys. Rev. Lett. **27**(25), 1719–1721 (1971).
18. J. Fitzpatrick, R. Malt, and F. Spaepen, "Percolation theory and the conductivity of random close packed mixtures of hard spheres," Phys. Lett. A **47**(3), 207–208 (1974).
19. S. Kirkpatrick, "Percolation and conduction," Rev. Mod. Phys. **45**(4), 574–588 (1973).
20. J. van de Groep, P. Spinelli, and A. Polman, "Transparent conducting silver nanowire networks," Nano Lett. **12**(6), 3138–3144 (2012).
21. L. Hu, H. Wu, and Y. Cui, "Metal nanogrids, nanowires, and nanofibers for transparent electrodes," MRS Bull. **36**(10), 760–765 (2011).
22. S. Xie, Z. Ouyang, B. Jia, and M. Gu, "Large-size, high-uniformity, random silver nanowire networks as transparent electrodes for crystalline silicon wafer solar cells," Opt. Express **21**(103), A355–A362 (2013).
23. M. Rycenga, C. M. Cobley, J. Zeng, W. Li, C. H. Moran, Q. Zhang, D. Qin, and Y. Xia, "Controlling the synthesis and assembly of silver nanostructures for plasmonic applications," Chem. Rev. **111**(6), 3669–3712 (2011).
24. D. Y. Choi, H. W. Kang, H. J. Sung, and S. S. Kim, "Annealing-free, flexible silver nanowire-polymer composite electrodes via a continuous two-step spray-coating method," Nanoscale **5**(3), 977–983 (2013).
25. W. L. Barnes, A. Dereux, and T. W. Ebbesen, "Surface plasmon subwavelength optics," Nature **424**(6950), 824–830 (2003).
26. M. Aryal, J. Geddes, O. Seitz, J. Wassei, I. McMackin, and B. Kobrin, "Sub-Micron Transparent Metal Mesh Conductor for Touch Screen Displays," in SID Symposium Dig. Tech. Pap. **45**(1), 194–196 (2014).
27. M. G. Kang and L. J. Guo, "Nanoimprinted Semitransparent Metal Electrodes and Their Application in Organic Light-Emitting Diodes," Adv. Mater. **19**(10), 1391–1396 (2007).
28. M. G. Kang, M. S. Kim, J. Kim, and L. J. Guo, "Organic solar cells using nanoimprinted transparent metal electrodes," Adv. Mater. **20**(23), 4408–4413 (2008).

1. Introduction

Patterned metallic layers gained interest as transparent electrodes for optoelectronic devices such as displays, solar cells, light emitting diodes, touch screens and smart windows in the last decade [1–8]. Variety of metallic patterns – pores, honeycombs, triangles and wires – were proposed and studied in details [9–12]. Multiple studies show that an open area dominates the transmittance of metallic patterned structures [13, 14]. For instance, the *Al* wired electrode reach around 90% transmittance, while the porous configuration exhibits only 80% at sheet resistance of 5 Ohm/sq [15]. Furthermore, materials with stronger plasmonic response show higher optoelectronic performance: as an example *Ag* nanoporous layers possess 8% higher average transmittance in visible wavelength range at sheet resistance of 3 Ohm/sq compared to identical *Al* layers [10, 15].

However, an impact of nano- and microscale patterns on the optoelectronic performance of metallic layers is poorly studied. Here we theoretically analyzed nano-/microscale porous and wired configurations for two materials – *Ag* and *Al* – possessing different plasmon response in visible wavelength range. We showed that *Ag* nanoporous/nanowired layers exhibit up to 20% higher transmittance due to stronger surface plasmon (SP) resonance, while within microscale the optoelectronic performance become comparable for both metallic layers and depends solely on its permittivity and conductivity. Moreover, the microscale *Ag* and *Al* layers exhibit up to 5% higher average transmittance.

2. Methodology

Figure 1 shows the geometrical models for the porous and wired metallic layers on the glass substrate. Pores and wires were arranged uniformly with interpore/interwire distance *a* and diameter of pore *d*. The simulation area was cut to unit cell, which size along *X* and *Y* axes

was set to the distances a and $a \times \sqrt{3}$ for hexagonally arranged porous layers [Fig. 1(a)] and distance a for wired layers [Fig. 1(b)].

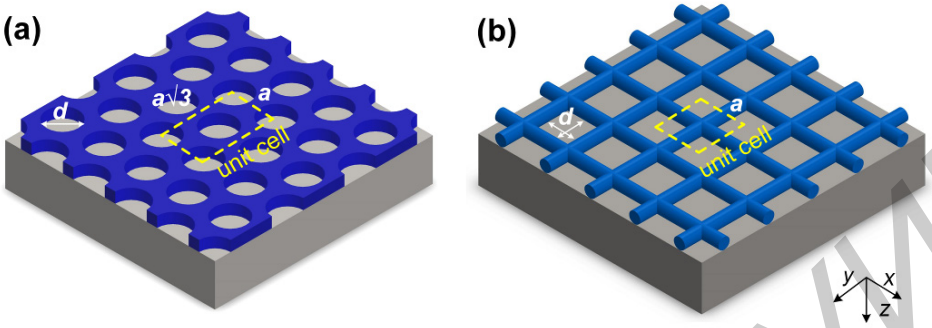

Fig. 1. Geometrical models for the porous (a) and wired (b) metallic layers on the glass substrate. Yellow dash rectangles are the unit simulation cells, which equal to $a^2 \times \sqrt{3}$ and a^2 for the pores and wired arrangements, respectively.

The optical properties were simulated using the finite-difference time-domain method which is commercially available within Lumerical software [16]. The incident light ranged in the visible spectrum was distributed along Z axis. The periodic boundary conditions and perfectly matched layers were applied perpendicular and parallel to Z axis, respectively. Mesh size was set to 10, 10 and 5 nm in X, Y, and Z directions, respectively.

The sheet resistance was calculated by the percolation model in accordance to [17–19], which is given by the following equation:

$$R_{sh} = \frac{1}{h\sigma_0 \left(\phi_f - \phi_{crit}\right)^t}, \qquad (1)$$

where σ_0 is the conductivity of metal, ϕ_f is the volume fraction of patterned metal layer, ϕ_{crit} is the volume fraction threshold when the patterned layer changes from insulator to conductor, h is the thickness of the metal layer and t is the critical exponent. Above mentioned models were successfully applied by our group in [10, 12, 15].

3. Results and discussion

Metallic patterns possess SP response in specific wavelength range, which depends on material and geometrical parameters of patterns. We chose two metals with different SP response in the visible spectrum: *Ag* with strong SP resonance from 400 to 700 nm and *Al* with weak SP response from 400 to 500 nm [20]. Thickness of the layers was set to 60 nm in order to represent the common experimental studies [21–24]. We selected the interpore/interwire distances a from 200 nm to 30 μm aimed to investigate the optoelectronic properties of micro- and nanoscale configurations. Ratio of diameter d to distance a changed from 20% to 100%; i.e. from structure close to bulk configuration to structure with near zero conductivity.

Figure 2 shows the average transmittance in the visible spectrum for *Ag* and *Al* porous layers against the interpore distance a and ratio d/a. Two regions – one from 200 to 800 nm wavelength (nanoscale) and another from 800 nm to 5μm (microscale) – illustrate different behavior. Within the *nanoscale* region *Ag* porous layers demonstrate up to 20% higher average transmittance in comparison to *Al* layers; major difference takes place for the ratio d/a from 40 to 90%. In the *microscale* region the average transmittance between *Ag* and *Al* layers differs by less than 2%. Such behavior results from distinct impact of SP response on the transmittance, viz. that the energy of SPs decays exponentially over its propagation path [25]. SPs reach the bottom side of the nanoscale structure and then re-radiate into light

enhancing the transmittance. In the microscale structure the energy of SPs reduces significantly at the bottom side due to long propagation path and negligibly influence on the transmittance.

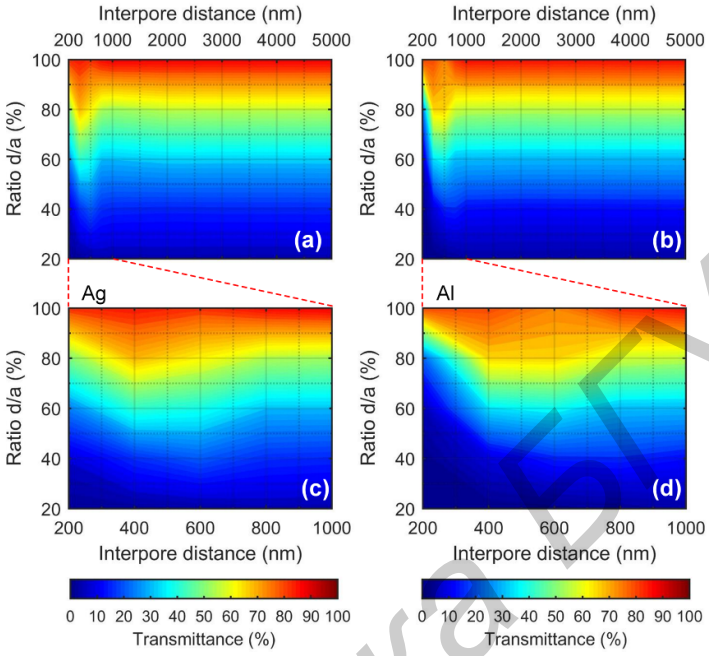

Fig. 2. The average transmittance in the visible spectrum for *Ag* (a, c) and *Al* (b, d) *porous* layers against the interpore distance *a* and ratio *d/a*.

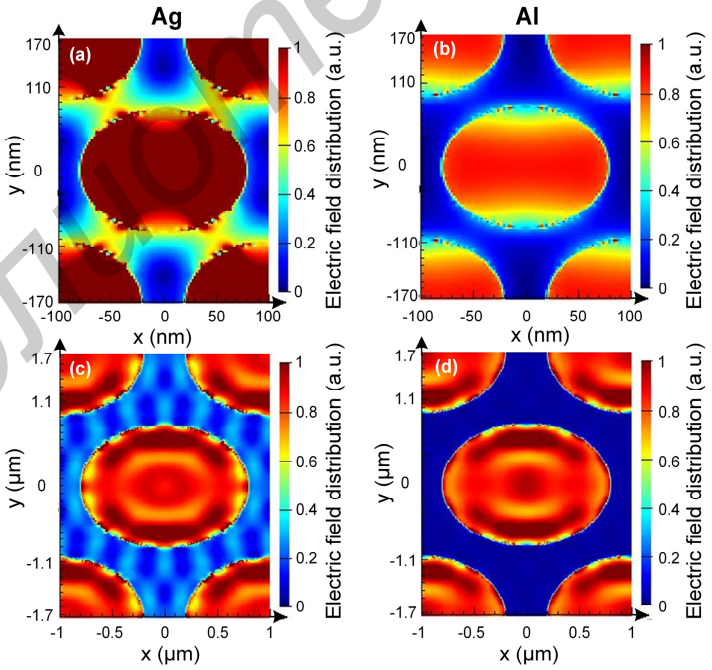

Fig. 3. The calculated electric field distribution for nano- (a = 200 nm) and microscale (a = 2 μm) *Ag* (a, c) and *Al* (b, d) layers at 550 nm wavelength.

Figure 3 illustrates the calculated electric field distribution for nano- (a = 200 nm) and microscale (a = 2 μm) *Ag* and *Al* layers at 550 nm wavelength. The nanoscale *Ag* layer possesses strongest electric field along metal, while at a = 2 μm the electric filed decreases four times. Both nano- and microscale *Al* layers demonstrate negligible electric field along metal compared to *Ag* layers. Thus, in microscale layers the transmittance depends solely on material permittivity and conductivity.

Ag and *Al* wired layers demonstrate similar effect as shown in Fig. 4: *Ag* outperforms *Al* up to 20% average transmittance in case of nanoscale layers, while within the microscale region the average transmittance differs by less than 2%.

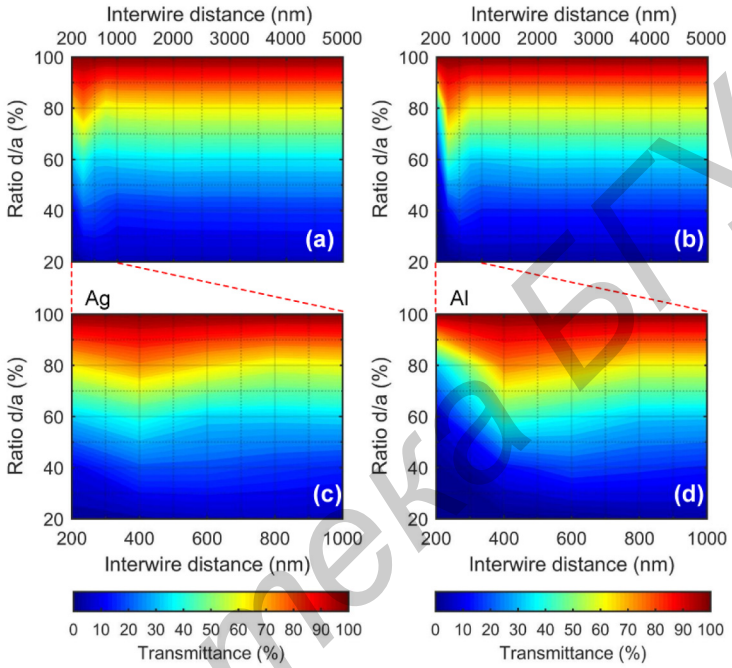

Fig. 4. The average transmittance in the visible spectrum for *Ag* (a, c) and *Al* (b, d) *wired* layers against the interwire distance a and ratio d/a.

Figure 5 shows the average transmittance in visible spectrum against the sheet resistance for nano- (a = 200 nm) and microscale (a = 2 μm) porous *Ag* and *Al* layers. *Ag* nanoporous layers possess the average transmittance of 77% at the sheet resistance of 5 Ohm/sq, while *Al* layers obtain close average transmittance only at 50 Ohm/sq. This difference results from both higher transmittance of nanoscale *Ag* layer and bulk conductivity of *Ag* ($\sigma_0 = 6.3 \times 10^7$ S/m) compared to *Al* ($\sigma_0 = 3.5 \times 10^7$ S/m). At microscale range the average transmittance of *Ag* layers becomes 82% at the sheet resistance of 5 Ohm/sq, while *Al* layers obtain close average transmittance at the sheet resistance 12.5 Ohm/sq. This difference comes mainly from higher bulk conductivity of *Ag* compared to *Al* and slightly higher transmittance of microscale *Ag* layers. The microscale *Ag* and *Al* layers exhibit up to four times lower sheet resistance at given average transmittance. Moreover, microporous layers show 5% higher average transmittance due to larger open area of micropores.

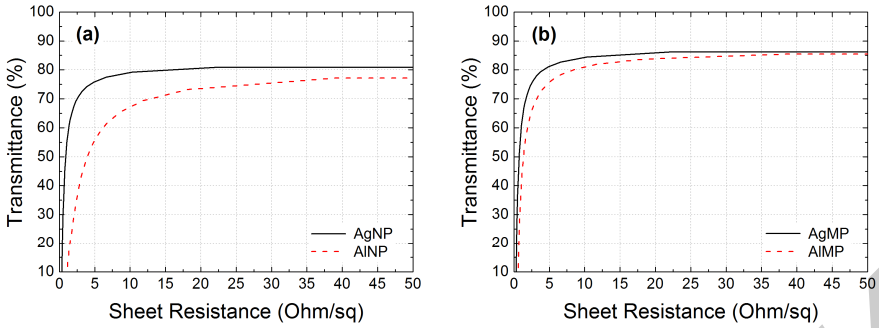

Fig. 5. Average transmittance against sheet resistance for nano- (a) and microscale (b) *porous* *Ag* and *Al* layers. The interpore distance *a* = 200 nm and 2 μm for nano- and microscale configurations, respectively.

Figure 6 shows that *Ag* and *Al* wired layers demonstrate similar tendency: (i) *Ag* nanowired layers possess the average transmittance of 88% at the sheet resistance of 5 Ohm/sq, while *Al* layers obtain close average transmittance only at 35 Ohm/sq; (ii) at microscale range the average transmittance of *Ag* layers becomes 92% at the sheet resistance of 5 Ohm/sq, while *Al* layers obtain close average transmittance at the sheet resistance of 9 Ohm/sq; (iii) microwired layers show 4% higher average transmittance due to larger open area.

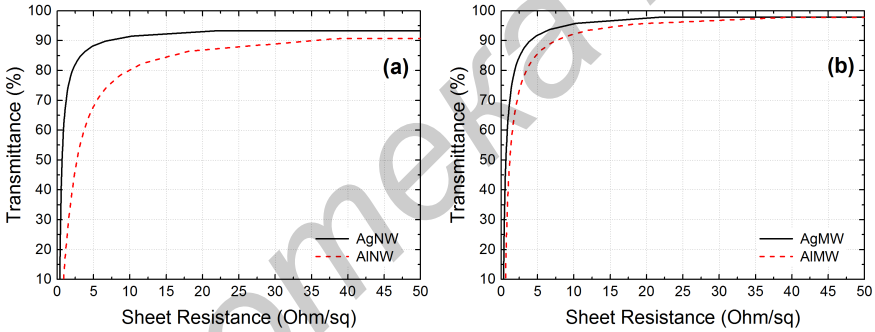

Fig. 6. Average transmittance against sheet resistance for nano- (a) and microscale (b) *wired* *Ag* and *Al* layers. The interpore distance a = 200 nm and 2 μm for nano- and microscale configurations, respectively.

Figure 7 shows the difference in average transmittance between *Ag* and *Al* layers against interpore/interwire distance *a* at fixed sheet resistance of 5 Ohm/sq. *Ag* layers exhibit from 20.2 to 6.5% higher transmittance at distance *a* from 200 to 600 nm, respectively. Further increment of the distance *a* affects the difference in the average transmittance between *Ag* and *Al* layers significantly less: *Ag* layers exhibit from 6.5 to 5% higher transmittance at the distance *a* from 600 nm to 30 μm. Close experimental results for nano- and microscale wired *Ag* and *Al* layers with distance were demonstrated in [26–28]. Large difference in transmittance – 20.2% at distance *a* = 200 nm – indicates that only *Ag* porous/wired layers can suit most optoelectronic aplications. Therefore, the metallic patterned layers with stronger SPs response possess higher optoelectronic performance at nanoscale patterns, while at microscale patterns their performance depends solely on permittivity and conductivity of micropatterned metallic layers.

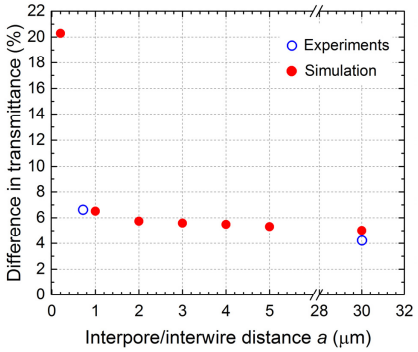

Fig. 7. Difference in average transmittance between *Ag* and *Al* layers against interpore/interwire distance *a* at fixed sheet resistance of 5 Ohm/sq. Experimental results from [26–28].

4. Conclusion

We theoretically studied the optoelectronic properties of nano-/microscale porous and wired *Ag* and *Al* layers. Both nanoporous and nanowired *Ag* layers show up to 20% higher average transmittance due to stronger SP response over the whole visible spectrum. However, at the microscale patterns the difference in average transmittance between *Ag* and *Al* layers becomes less than 5%. Moreover, the microscale *Ag* and *Al* layers exhibit up to 5% higher average transmittance. The obtained results allow to estimate the impact of the pattern size of metallic transparent conductive layers on its optoelectronic performance for various optoelectronic applications, such as displays, solar cells, light-emitting diodes, smart windows, and other devices.

Acknowledgment

This project is supported by National Research Foundation of Singapore (No. NRF-CRP11-2012-01).